Sigma J Eng Nat Sci, Vol. 43, No. 1, pp. 96–106, February, 2025

Sigma Journal of Engineering and Natural Sciences
Web page info: https://sigma.yildiz.edu.tr
DOI: 10.14744/sigma.2025.00008

Research Article

Comparative evaluation of plane-bending fatigue behavior of resistance spot-welded joints in dual-phase steels of different strength levels

Muhammed ELİTAŞ[1,*], Bilge DEMİR[2], Mustafa GÖKTAŞ[2]

[1]*Department of Mechanical Engineering, Bilecik Şeyh Edebali University, Bilecik, 11100, Türkiye*
[2]*Department of Mechanical Engineering, Karabuk University, Karabuk, 78050, Türkiye*

ARTICLE INFO

Article history
Received: 18 November 2023
Revised: 23 December 2023
Accepted: 24 January 2024

Keywords:
Automotive Sheet Steel; Fatigue Fracture Mode; Fatigue Test; Resistance Spot Welding; Weld Nugget

ABSTRACT

This study attempted to explain comparatively the plane-bending fatigue behaviors of resistance spot-welded junctions using commercial DP600 and DP1000 automotive steel sheets having different strength levels. In addition, the fracture modes of the samples were evaluated and interpreted according to SEM examinations. First, standard junction samples were produced via resistance spot welding using two weld currents and three different electrode pressures. Microimage analysis and plane-bending fatigue tests were carried out on the samples. The maximum strain energy hypothesis was applied experimentally to obtain the fatigue test load force, and plane-bending fatigue stress values were obtained. Unlike the load/cycle graphics generally presented in the literature, Wohler S-N graphics were drawn, making this study different from others. The results of this study demonstrated that an increase in welding current led to an increment in fatigue strength. A significant relationship was also observed between weld nugget attributes and fatigue strength. Moreover, some intriguing results were obtained, e.g., the low-cycle fatigue life of the DP600 samples exhibited lower fatigue strength than that of the DP1000 samples; however, the high-cycle fatigue life of the DP600 samples showed higher fatigue strength than that of the DP1000 samples.

Cite this article as: Elitaş M, Demir B, Göktaş M. Comparative evaluation of plane-bending fatigue behavior of resistance spot-welded joints in dual-phase steels of different strength levels. Sigma J Eng Nat Sci 2025;43(1):96–106.

INTRODUCTION

Looking over the last forty years, we see that the most effective developments in transport have been gained in materials. Advanced high-strength steels (AHSSs), particularly dual-phase steels, have been playing a major and crucial role in terms of improved savings of both life and fuel. Because of the effective properties of these steels, today's vehicles are stronger, safer, more economical, and more comfortable. Above all, when evaluating all crash conditions, these properties could be said to exhibit better crashworthiness, better crash energy absorption, better fatigue strength, and low-cycle fatigue [1].

Why are dual-phase steels preferred over other AHSSs in the automotive industry? The answer to this question is that dual-phase steels are economical and have superior

*Corresponding author.
*E-mail address: muhammed.elitas@bilecik.edu.tr

This paper was recommended for publication in revised form by Editor-in-Chief Ahmet Selim Dalkilic

properties such as a good strength-ductility relationship, formability, etc. [2]. Dual-phase steels, with their advantageous properties, continue to make future advances. Currently, dual-phase steels are high- and ultra-high-strength steels (on a scale of 450−1200 + MPa) [3,4]. Indeed, dual-phase steels have been developed especially for use as sheet metal and for automotive applications. Automotive body production uses sheet steel. This production's preferred welding method is resistance spot welding (RSW) [5,6]. This method is favored, particularly in the body construction of automobiles, because it is widely used, fast, and appropriate for robotic manufacturing automation.

Furthermore, RSW does not require additional materials like other welding methods [7–10]. It is common knowledge that an automobile body may comprise more than 5000 resistance weld spots. Therefore, RSW is a widespread and important welded joining method, especially in automotive body production, and thus continues attracting researchers' attention to dual-phase steels [11].

Crash performance is among the most important criteria for welded joints and automobile body production sheets. Like its other attributes, the fatigue performance of dual-phase steel and its resistance spot-welded parts are also very important and play a key role in a crash [12–14]. The geometry of the nugget is one of the important factors having a huge effect on the fatigue performance of resistance spot-welded parts [8,15]. One reason may be the notch effect of electrode indentation in the event of a crash. The materials' notch and surface conditions significantly affect their mechanical properties, particularly fatigue strength [3,16]. Unfortunately, failures may not be entirely escapable, especially in manufacturing and RSW [17]. All vehicles are exposed to dynamic loads during working and service circumstances. As with all areas of weakness, the problem of auto-body fatigue performance must be solved because it ends in brittle fracture. Therefore, fatigue performance continues to be among the main contemporary topics studied worldwide [18].

Today, advanced high-strength steels, particularly DP600 and DP1000 steel sheets, are very important materials in manufacturing automotive body sheet parts, considering the amount used, their strength, and their formability properties [18]. As mentioned before, the performance under dynamic conditions of the auto body joined by welding is particularly crucial and needs detailed research [3,7,13]. It is very important to provide a new technique that helps to solve problems and develop all properties of the materials used in the manufacturing of vehicles. Some important literature based on the work conducted on fatigue properties of RSW welded dual-phase steels is discussed here. Soomro et al. [19] investigated the effects of double pulse welding on the fatigue behavior of DP590 steel resistance spot weld. They determined that specimens made via the double pulse RSW method had more cycles (about 10-23%) than those made via single pulse RSW method. Janardhan et al. [20] studied the influence of work hardening on the fatigue behavior of RSW welded DP600 steel. They stated that the prestraining of DP600 steel sheets has no substantial influence on the fatigue strength of spot-welds, and the joints fail from the interfacial region of HAZ. Kishore et al. [21] examined RSW welded DP600 and interstitial free (IF) steel fatigue behavior. They obtained that the fatigue specimen failed from the HAZ of the IF steel side with transgranular striations on the fracture surface. Ghanbari et al. [22] investigated the effects of RSW parameters on the fatigue behavior of ferrite martensite dual-phase steel and hybrid joints. The results showed that the effect of electric current on the fatigue life of joints is more than that of other parameters, and the adhesive on the hybrid joints also significantly affects the increase of its fatigue life and fatigue strength. Xie et al. [23] carried out fatigue characteristics of DP780 steel spot welding joints with different static fracture modes. They found that applied load, microhardness gradient in HAZ, and inclined angle on the faying surface caused by deformation influence the fatigue life. Ordonez et al. [24] studied the overloading effect on the fatigue strength in RSW joints of DP980 steel. They observed that the stress concentration factor produced by the spot-welding geometry decreased the fatigue life behavior. Ordonez Lara et al. [25] also investigated the fatigue life of RSW welded DP590 and DP980 steels. They obtained Wöhler curves at a constant load ratio to determine the fatigue life. They stated that failures of the joints were initiated in the nugget zone. In the open-access literature, the studies on RSW junctions of advanced steel have generally focused on rotational fatigue testing assisted by tensile-compression fatigue tests. However, RSW welded specimens are not only subject to tensile-compression or rotational fatigues. It can also be subject to plain-bending fatigue. Unlike in previous investigations, the present study sought to explain the plane-bending fatigue behaviors of DP600 and DP1000 automotive sheet steel by testing resistance spot-welded samples using both calculation and experimental methods and comparing the results.

Moreover, no study was found in the open-access literature that compared DP600 and DP1000 steels or calculated the plane-bending fatigue stress and the fatigue performance of their RSW weld joints. In addition, fatigue results have generally been given as load, and the use of the maximum energy hypothesis in stress calculations has not been observed. Also, the effects of welding parameters such as welding current and welding time on fatigue properties were examined, and very few studies were found on the effect of electrode pressure. So, this study concentrates on the impact of different welding current and electrode pressure parameters of DP600 and DP1000 sheets joining in RSW. Hence, the influence of process parameters plays an important role in acquiring good-quality welding. Finding appropriate welding parameters for RSW is a very complex case. A small modification of any parameter affects weld quality, which enhances the failure rate. As a result, plain bending fatigue behavior was investigated in detail. Welding

parameters were optimized in resistance spot welded joints of DP steels, and ideal welding parameters were determined for a safe and reliable design in this study.

EXPERIMENTAL METHODS

Materials

Commercial DP600 and DP1000 steel sheets with dimensions of 250×250×1mm and 500x500x1.2 mm were obtained from TOFAŞ Otomotiv Inc. in Bursa, Türkiye. Then, samples with 100x30 mm dimensions were prepared by cutting them with guillotine shears. The SPECTROLAB LAVFA18A spectrometer with 230VAC heat input, 50Hz frequency, and 2500VA power capacity was used to determine the chemical compositions. Microstructural analysis was performed using a Nikon Epiphot 200 optical microscope. Specimens for microstructural analysis were ground (polished) with 120, 240, 360, 600, 800, 1000, 1200, 1500, and 2000 mesh SiC abrasives, 3 µm and 1 µm diamond paste solutions, respectively, and etched in 2% Nital solution (2% Nitric acid + 98% Methanol). Their chemical compositions are given in Table 1, and their microstructures in Figure 1. As can be seen, these are classic dual-phase steel structures having different ferrite/martensite phase contents. Essentially, this difference also provides the difference in strength and ductility properties. The ferrite phase is light-colored, whereas the martensite particles are dark (Figure 1). When Figure 1 is examined, it was observed that DP600 steel contains a high amount of ferrite and a small amount of martensite. On the contrary, DP1000 steel contains a small amount of ferrite and a high amount of martensite.

Resistance Spot Welding

The RSW weld samples were prepared by shearing the steel sheets according to EN ISO 14273 standard. The RSW application was carried out in the Baykal SPP60 welding machine (which is located at Karabuk University) using 8-mm flat conical tip electrodes. The technical properties of the welding machine included a phonematic force application, a timer, and changeable weld currents and weld pressures, with a capacity of 60kW. A specially prepared wood fixture was used during the RSW process to secure the overlapped specimens. The welding time unit used was the cycle (1 cycle = 0.02 s). The RSW process used in the study was carried out with the welding parameters determined by preliminary experiments.

Additionally, previous studies were used to determine the optimal welding parameters regarding weld quality and maximum strength [16,17]. So, resistance spot-welded samples were produced by using two different weld currents (5 kA and 7 kA) and different weld pressures (3-5 bar) (Table 2). These parameters were the same for both DP600 and DP1000 overlapped sample groups. Three samples were produced for each parameter. RSW samples were 30 mm in width and 165 mm in length (Figure 2). Nugget diameter measurements were performed using a digital caliper. The nugget diameter is shown schematically in Figure 3 [10]. Average nugget diameter (d_a) values for different welding parameters were calculated using Equation (1)[10,26].

$$d_a = \frac{d_1 + d_2}{2} \quad (1)$$

Table 1. Chemical composition of DP600 and DP1000 steels (wt.%)

Material	C	Si	Mn	S	Cr	Ni	Al	Ti	V	Fe
DP600	0.077	0.253	1.86	0.006	0.177	0.012	0.127	0.002	0.004	Balance
DP1000	0.136	0.203	1.57	0.003	0.022	0.039	0.044	0.001	0.009	Balance

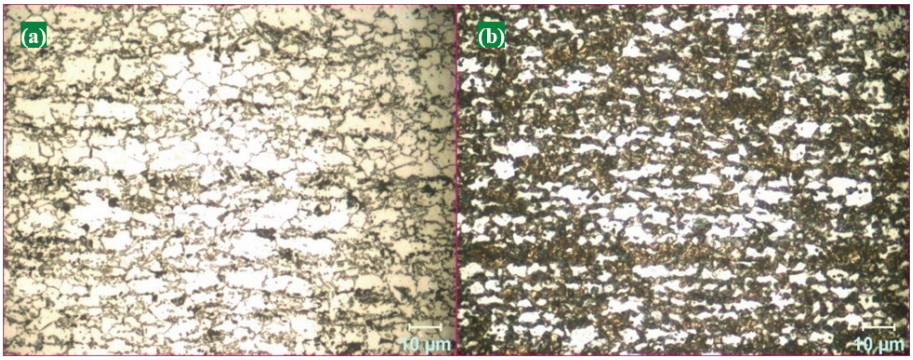

Figure 1. Microstructure of base materials (a) DP600, (b) DP1000.

Table 2. RSW welding parameters

Welding current (kA)	Electrode pressure (bar)	Downtime (cycle)	Squeeze time (cycle)	Welding time (cycle)	Holding time (cycle)	Separation time (cycle)
5&7	3&4&5	15	35	20	10	15

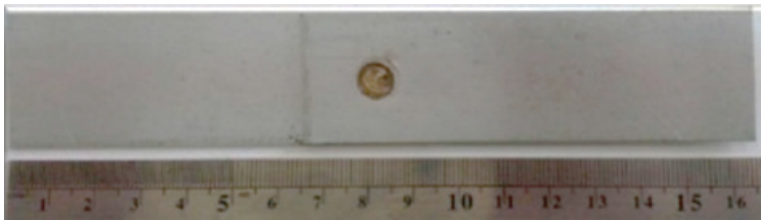

Figure 2. RSW sample.

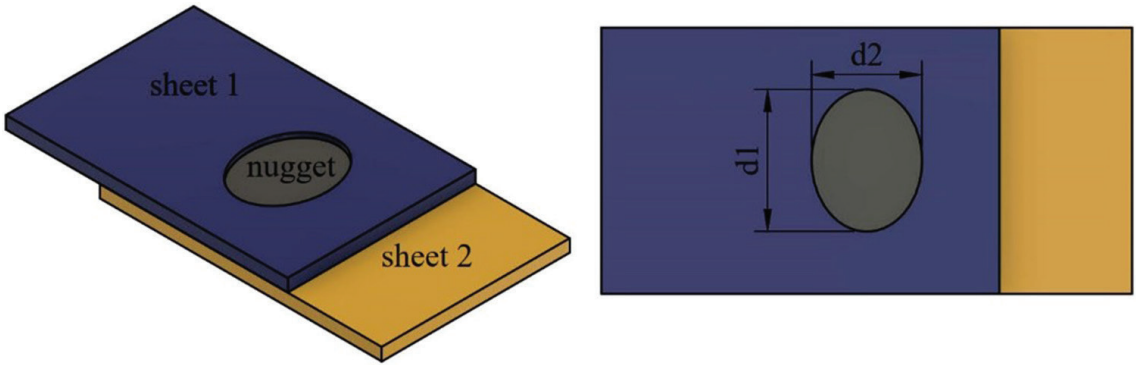

Figure 3. Schematic view of nugget diameter [10].

Fatigue Test

The plane-bending fatigue test machine was supplied by Turkyus Limited Company in Bursa, Türkiye, within the scope of the Karabuk University scientific research project. The fatigue test machine and schematic test procedure are shown in Figure 4. Plane-bending fatigue tests were performed on overlapping samples joined by RSW using two different weld currents and three different weld pressures, such as 3, 4, and 5 bars. These parameters and the samples used in this study were selected and applied according to the highest tensile load-bearing capacity values cited in our previous study results [7,15]. Plane bending fatigue tests were performed at different displacement amplitude strain values (11, 12, 13, 14, 15, and 16 mm) and a constant frequency value (10 Hz) to 3 samples for each parameter. The arithmetic average of the results obtained for each parameter was taken. Experimentally obtained load-cycle values were converted to stress-cycle values by performing calculations according to the maximum strain energy hypothesis.

Table 3. Plain bending fatigue test parameters

Material	Welding Parameters	Amplitude values (mm)	Frequency (Hz)
DP600	5kA-5bar	11-16	10
DP600	7kA-4bar	11-16	10
DP1000	5kA-3bar	11-16	10
DP1000	7kA-3bar	11-16	10
DP600	-	11-16	10
DP1000	-	11-16	10

Consequently, fatigue test results could be expressed as Wohler S-N (fatigue stress/number of cycles) graphics. Plain bending fatigue test parameters are given in Table 3. In addition, weld fracture surfaces were examined with CARL ZEISS ULTRA PLUS GEMINI FESEM device.

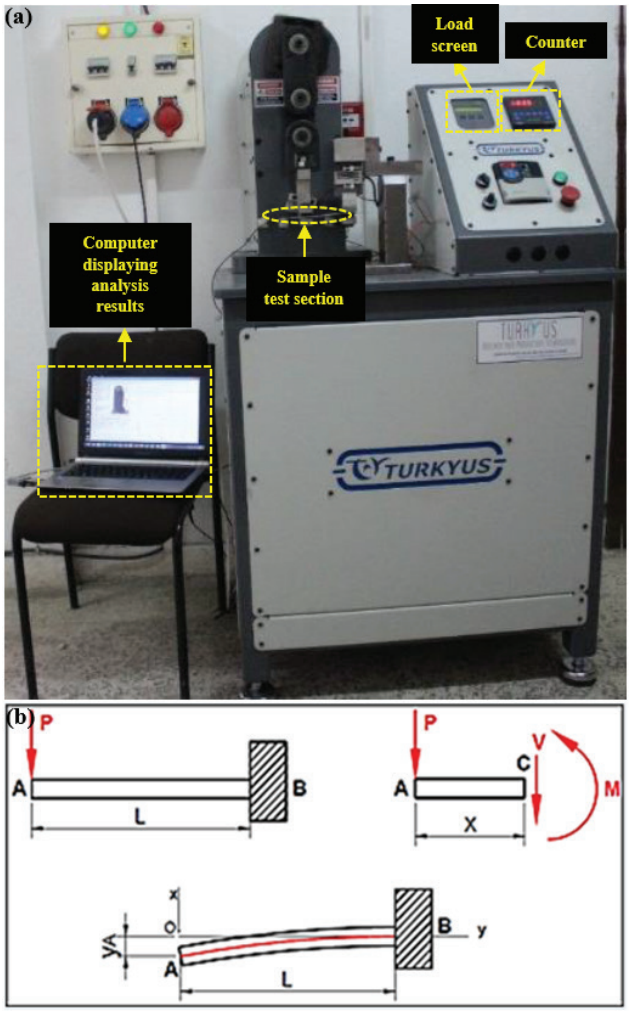

Figure 4. Fatigue test setup (a) fatigue test machine, (b) schematic test procedure.

RESULTS AND DISCUSSION

Analysis of Plane-Bending Fatigue Behaviors

The schema in Figure 4b shows the dynamic conditions of this study, with P representing the force, L the distance between two holding grips, M the moment, and y_A the maximum point in displacement. The maximum plane-bending fatigue stresses were calculated using Equations (2)-(8). The applied plane-bending force (average force value until the sample breaks) was used. As these conditions continued, maximum plane-bending moments were formed at the tips of the samples. These moments were previously calculated by multiplying the applied force (F) by the distance (d) between the force-applying head and force-applied point (force multiplied by the force arm) (Equation 2) [27], and the effect of the formed force on the sample was estimated at its mid-point; however, the weight of the samples was not considered in this calculation. The force arm length was calculated as 74 mm with these conditions. The plane-bending moments of the samples were calculated using Equation (2).

$$M_e = F \times d \tag{2}$$

Equation (3) shows the samples' bending moment strength. The plane-bending moment (M_e) obtained via Equation (2) was divided by the bending moment strength (W), yielding the bending stress at the investigated points (Equation 4) [27].

$$W = \frac{b \times h^2}{6} \tag{3}$$

$$\sigma_e = \frac{M_e}{W} \tag{4}$$

The force (F) on the sample was calculated by using the bending stress from Equation (4) and multiplying it by the top surface area of the sample. Shear stress was then obtained by dividing this force by the vertical cross-sectional area (A) (Equation 5).

$$\tau_k = \frac{F}{A} \tag{5}$$

The maximum strain energy hypothesis was used to find the resultant stress, which is appropriate for ductile materials subjected to dynamic force. That is shown in Equation (6) [27].

$$\sigma_R = \sqrt{{\sigma_e}^2 + 3{\tau_k}^2} \tag{6}$$

Using Equation (6) above, the resultant stress was calculated for two samples of different thickness (t): DP600 (t = 1 mm) in Equation (7) and DP1000 (t = 1.2 mm) in Equation (8), respectively.

$$\sigma_{DP600} = \sqrt{\left(\frac{F \times 74}{5}\right)^2 + 3 \times \left(\frac{F}{30}\right)^2} \tag{7}$$

$$\sigma_{DP1000} = \sqrt{\left(\frac{F \times 74}{7.2}\right)^2 + 3 \times \left(\frac{F}{36}\right)^2} \tag{8}$$

The stress, σ-cycle number, and N graphs generated based on the stress values calculated using Equations (7) and (8) are shown in Figure 5. The fatigue life of the RSW samples decreased as the shear component of the loading conditions increased due to an increase in amplitude value (grip tidal distance)[19,21,28]. So, it was observed that the fatigue life of the RSW DP600 and DP1000 steel sheet samples decreased with the increase of amplitude values from 11 to 16 mm.

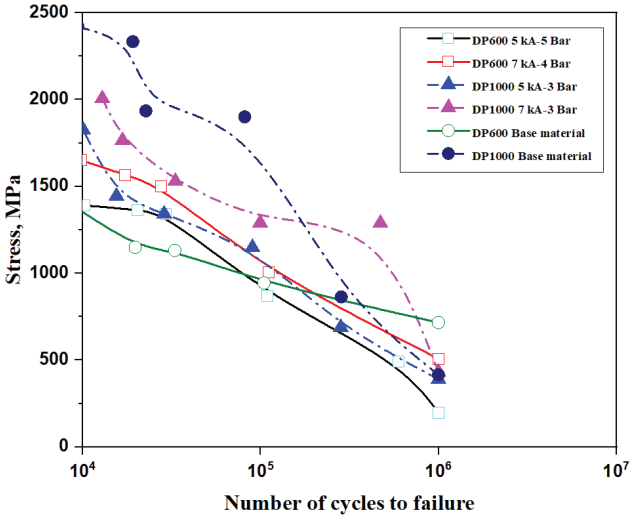

Figure 5. Fatigue curves of original and RSW DP600 and DP1000 samples.

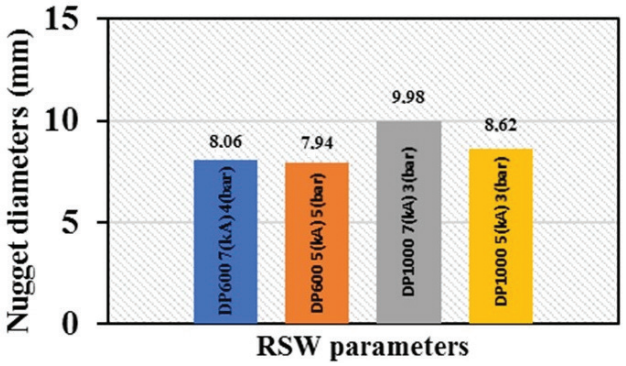

Figure 6. Nugget sizes obtained at different welding parameters.

It could be understood that the heat input varied depending on the welding parameters. As the heat input increased, the RSW nugget size also increased. A direct proportional relationship existed between the samples' nugget size, strength, and fatigue life-strength. As the weld nugget size increased, the stress concentration factor around the notch root decreased [19,29,30]. It was assumed that the fatigue performance of the resistance spot-welded samples had been mainly affected by their geometry rather than their material types or microstructures. Graphics showing the nugget size vs. weld parameters are given in Figure 6.

The decrease in the stress concentration factor increased the initial fatigue life [18,24,30–33]. In Figure 6, the RSW welded DP600 samples had two different welding parameters: 7 kA- 4 bar-8.06-mm nugget size and 5 kA-5 bar-7.94-mm nugget size. When considering this, the experiment showed that the samples with 7 kA-4 bar-8.06-mm nugget size parameters demonstrated better fatigue strength. For the DP1000 steel, 7 kA-3 bar-9.98-mm nugget size welding parameters yielded better fatigue strength than 5 kA-3 bar-8.62-mm nugget size parameters. It was observed that electrode pressure and welding current increased the weld nugget size. However, electrode pressure affected the weld nugget size more than the welding current.

While a 1 unit increase in welding current caused a 0.68 mm increase in weld nugget diameter (between 5kA-3 bar and 7 kA-3 bar), a 1 unit decrease in electrode pressure caused a 1.24 mm decrease in weld nugget diameter (between 5kA-5bar and 7kA-4 bar). Because with a 2-unit increase in welding current, the weld nugget size was expected to be 9.3 mm, but 8.06 mm was obtained. In other words, a 1 unit decrease in electrode pressure resulted in a 1.24 mm decrease. In this context, it can be said that the effect of electrode pressure on the weld nugget size is approximately 82% higher than the welding current. Generally, the results obtained in this study have confirmed the direct relationship between the weld nugget size and fatigue strength. In Figure 5, samples of the same materials obtained using different welding parameters show similar fatigue behavior for low-cycle fatigue. The fatigue crack propagation rate in low-cycle fatigue (at high amplitude values) is controlled by the microstructure and strength of the base metal. In high-cycle fatigue (at low amplitude values), the fatigue crack propagation rate is independent of the microstructure and strength of the base metal. That is attributed to the change in the failure location during cyclic loading compared to static loading [20]. Geometric factors such as weld nugget size affect the fatigue crack propagation rate [20,31,34,35]. In high-cycle fatigue, at the parameters of 5 kA-5 bar in the DP600 steel, fracture occurred at approximately 600,000 cycles, whereas the fatigue limit was reached at 7 kA-4 bar.

However, Soomro et al. [19] found that the fatigue limit was reached at the parameters of 7.5 kA-4 kN. In addition, Janardhan et al. [20] and Kishore et al. [21] stated that the fatigue limit was reached at 8 kA-3.8 kN and 7 kA-7.45 kN, respectively. When the results are compared, the fatigue limit was reached at a lower welding current value in the current study. In the DP1000 steel, samples fractured at approximately 300,000 cycles for the parameters of 5 kA-3 bar, whereas at the parameters of 7 kA-3 bar, they fractured at approximately 500,000 cycles. However, Ordonez et al. [24] obtained that the failure happened about 100,000 cycles for RSW DP980 steel. In the current study, it was observed that fracture occurred at higher cycles. In this context, a contribution to the literature has been made. Also, when the results are evaluated in general, there are important developments, especially for the automotive industry. Because the majority of spot weld failures in automobiles occur due to cyclic loading in the form of vibrations [19]. So, fatigue behavior is one of the important factors in the automotive industry, and the results of current studies show

Table 4. High cycle fatigue results

Material	Welding Parameters	Nugget size (mm)	Number of cycles to failure	Fatigue limit strength (MPa)	Decrease according to base material strength (%)
DP600	5kA-5bar	7.94	600,000	198	72
DP600	7kA-4bar	8.06	Endurance	508	29
DP1000	5kA-3bar	8.62	300,000	389	6
DP1000	7kA-3bar	9.98	500,000	430	-
DP600	-	-	Endurance	716	-
DP1000	-	-	300,000	415	-

that it increases the life of the joint. In addition, the results of the current study will prepare a framework for future studies on plain bending fatigue in terms of the optimization of welding parameters.

Figure 5 also shows the comparative fatigue behaviors of DP600 (1 mm) and DP1000 (1.2 mm) automotive steel sheets. The DP1000 steel with higher tensile strength in low-cycle fatigue (at high amplitude values) exhibited higher fatigue strength values than the DP600 steel. Because DP1000 steel has a more martensitic structure than DP600 steel. Since the martensite phase is an important factor that increases hardness and tensile strength values, higher values were obtained in low-cycle fatigue.

On the other hand, in high-cycle fatigue (at low amplitude values), the DP600 steel demonstrated better fatigue strength. At approximately 300,000 cycles, the DP1000 steel fractured, whereas the fatigue limit had been reached for the DP600 steel. DP600 steel contains a higher amount of ferrite phase compared to DP1000 steel, which increases ductility. So, the ductility of DP600 steel is effective compared to the tensile strength of DP1000 steel [18].

Figure 5 shows that the fatigue limit of the 7 kA-4 bar RSW weld sample of the DP600 steel sheet was reached at the 508 MPa stress value, whereas the fatigue limit of the 5 kA-5 bar RSW weld sample of the same steel was reached at the 198 MPa. However, the RSW-welded 7 kA-3 bar samples of DP1000 reached the fatigue limit at a stress value of nearly 430 MPa, and the 5 kA-3 bar samples reached their fatigue limit at about 389 MPa. All fatigue limits for the DP600 and DP1000 base metal automotive steel sheets were nearly 716 MPa and 415 MPa, respectively. In the DP600, decreases of approximately 29% at the 7 kA-4 bar parameters and approximately 72% at the 5 kA-5 bar parameters were observed in the fatigue strength values of the automotive steel sheets after the RSW operation. In the DP1000 steel, the samples welded at parameters of 5 kA-3 bar showed a decrease of about 6% in the fatigue limit compared to that of the base material. Also, high cycle fatigue results are given in Table 4.

According to Holovenko et al. [36], after the RSW process, the notch effect caused by the RSW and the heterogeneous microstructure formed in the welding regions (the base metal, HAZ, and weld metal) could result in the reduction of fatigue life. They also reported that for a 1.8 mm DP1000 steel sheet, the fatigue life was essentially 570 MPa after RSW welding with parameters of 4 kN electrode force, 260 ms weld time, and 10 kA current, and that the fatigue life of the RSW junction of the DP1000 steel was reduced to 190 MPa. According to Onn et al. [12], the base metal fatigue life of a DP600 steel sheet with a 1.2-mm thickness had a stress value of nearly 255 MPa. Differences among fatigue life values reported by various studies could be attributed to several factors, such as the different geometry of the nuggets used in the calculation and differences in chemical composition of the DP sheet materials. Although the tensile properties of commercial DP steel are similar, chemicals in steel may differ according to the manufacturers and their expertise. Therefore, the fatigue life of the same quality of advanced steel could vary worldwide due to all the factors mentioned above.

Fatigue Fracture

Fracture takes place in two stages: initial formation and propagation of the crack. Metals display different types of fracture depending on the type of material, the applied load, the state of stress, and temperature. Brittle fracture is among the important types of fracture. It is the failure of a material with a minimum of plastic deformation. If the broken pieces of a brittle fracture are fitted together, the original shape and dimensions of the specimen are restored. A brittle fracture is defined as a fracture that occurs at or below the elastic limit of a material.

A fatigue fracture is a fracture that occurs under repeatedly applied stresses. It occurs at stresses well under the tensile strength of the materials. The tendency of fatigue fracture increases with the rise in temperature and a higher strain rate. Fatigue fracture occurs because of the microcracks on the surface of the material and results in the formation of dislocations near the surface. The micro-cracks act as points of stress concentration. For every cycle of stress application, the excessive stress facilitates the propagation of the crack. The crack grows slowly in ductile materials, and the fracture occurs rapidly. However, the crack grows to a critical size in brittle materials and spreads rapidly.

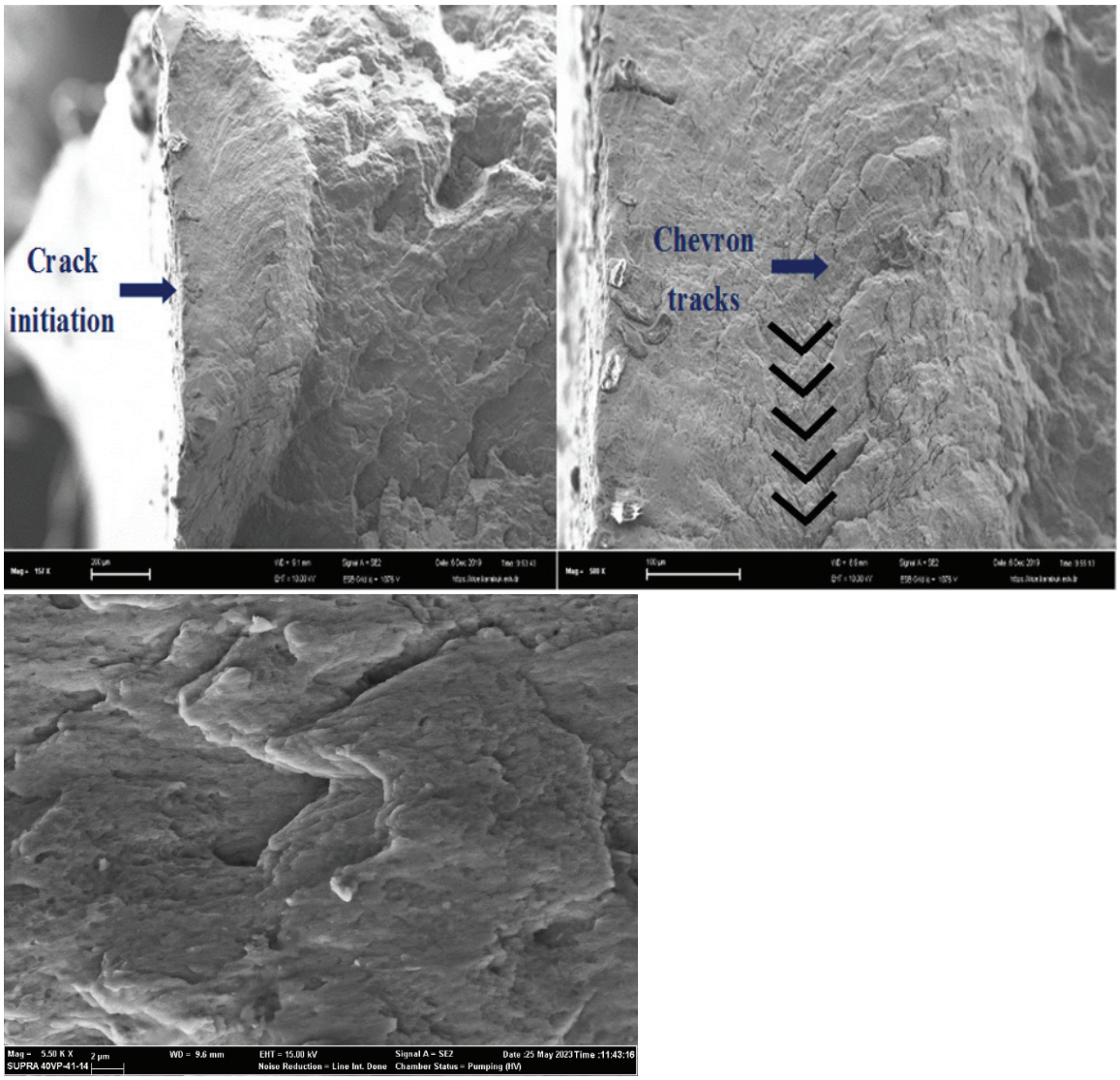

Figure 7. SEM images of the fracture surfaces.

When Figure 7 is examined, during dynamic plane bending, a chevron-fracture pattern was observed with general fatigue fracture, and explanations have been presented to understand this pattern. Chevron pattern is an important indicator of brittle fracture. The fracture may progress within the grain boundary or in the grain via the cleavage mechanism. A typical feature of fracture surfaces is the V-shaped chevron pattern (Figure 7b). Chevron marks indicate the starting point of the crack. The process of cleavage fracture consists of three steps in addition to nano conditions. First, plastic deformation produces dislocation pileups. Second, crack initiation occurs (Figure 7a), and finally, crack propagation leads to failure. A grainy or faceted texture, river marking and stress lines (chevron notches), and the absence of gross plastic deformation are distinct characteristics of brittle fracture surfaces.

In addition, it can be seen in Figure 7 that interfacial fracture mode occurred in the sample. The crack propagated through the nugget centerline in this failure mode, thus separating the joint into two pieces. The fracture surface of the sample exhibits torn bands (Figure 7c). It is well known that torn bands are characteristics of typical cleavage fracture [19,21]. The crack initiated from the notch and propagated rapidly through the nugget center. The load suddenly drops to zero level with little plastic deformation.

In mechanical fatigue, damage develops due to exposure to cyclic stresses over an extended period. It is worth noting that numerous classes of components (e.g., rotating equipment and pressure reduction valves) designed for alternating mechanical stresses are not usually subject to fatigue failure unless damaged by some other mechanism (e.g., foreign object impact damage or corrosion).

According to the open literature, fracture surfaces of interracially failed spot welds exhibit mainly cleavage fracture as well as small areas of ductile fracture. That follows the common brittle fracture in the hard bainitic/ martensitic microstructures found in the HAZ and weld nuggets of relatively high-alloyed DP or TRIP steels [18]. DP600 and DP1000 steels mainly contain a ferrite phase and a low proportion of martensite phase. However, after RSW, the weld zones mainly contain martensite phase, which causes brittleness. Therefore, brittle fracture mode was observed in all RSW samples.

In this fatigue fracture experiment, considering low- and high-cycle fatigue loads (Figure 4), very few crack nuclei were observed in the DP600 and DP1000 base materials. That means that the loading amplitude or stress concentration was minimal. In contrast, DP600 and DP1000 steel sheets developed multiple crack nuclei with RSW. Similar observations have been reported in the literature [17,18]. Ultimately, this was validated by the S-N diagram illustrated in Figure 5.

CONCLUSION

This study optimized plain bending fatigue behaviors with different welding currents and electrode pressure parameters. DP600 and DP1000 automotive sheet steels, widely used in the automotive industry in recent years to lighten vehicle weight, were joined by the resistance spot welding method. The following conclusions can be drawn:

- It has been observed that welding parameters, microstructure, and nugget diameter are important factors affecting bending fatigue behavior.
- Increasing amplitude values from 11 to 16 mm caused decreases in the fatigue life of both RSW-welded samples.
- A direct correlation was found between the fatigue strength and the weld nugget size. In the DP600 steel, fracture occurred at approximately 600,000 cycles, and the fatigue limit was reached (at 7.94 mm and 8.06 mm weld nugget sizes, respectively). In the DP1000 steel, samples fractured at approximately 300,000 and 500,000 cycles (at 8.62 mm and 9.98 mm weld nugget sizes, respectively).
- Samples of the same group showed similar fatigue behavior under low-cycle fatigue. However, under high-cycle fatigue, 7 kA-4 bar samples of DP600 steel and 7 kA-3 bar samples of DP1000 presented higher fatigue strength than the others.
- In contrast to low-cycle fatigue, the DP600 RSW-welded steel samples presented better fatigue life behavior in high-cycle fatigue than the DP1000 RSW-welded steel samples.
- There is a decrease in the bending fatigue strength of resistance spot welded samples compared to DP600 and DP1000 automotive sheet steels due to the notch effect formed in the weld nugget and the microstructure heterogeneity between the base metal, HAZ, and weld metal.
- Chevron marks and torn bands, an important indicator of brittle fracture, were observed in all samples in low-cycle and high-cycle fatigue.
- Experimental plain bending fatigue studies determined optimum welding parameters. To Compare the experimental study, finite element analysis results can be recommended for further research.

ACKNOWLEDGMENTS

This work was supported by the Scientific Research Projects Coordination Unit of Karabuk University (Karabuk, Turkey). Project Number: KBÜBAP-17-KP-463.

AUTHORSHIP CONTRIBUTIONS

Authors equally contributed to this work.

DATA AVAILABILITY STATEMENT

The authors confirm that the data that supports the findings of this study are available within the article. Raw data that support the finding of this study are available from the corresponding author, upon reasonable request.

CONFLICT OF INTEREST

The author declared no potential conflicts of interest with respect to the research, authorship, and/or publication of this article.

ETHICS

There are no ethical issues with the publication of this manuscript.

REFERENCES

[1] Elitas M. Effects of welding parameters on tensile properties and fracture modes of resistance spot welded DP1200 steel. Mater Test 2021;63:124–130. [CrossRef]

[2] Elitas M. Investigation of the fatigue behaviors of resistance spot welded advanced high strength automotive sheet steels (Doctorial thesis). Karabuk: Karabuk University; 2018. [Turkish]

[3] Maggi S, Scavino G. Fatigue characterization of automotive steel sheets. 11th International Conference on Fracture, Torino, Italy, vol. 1, 2005, p. 522–1.

[4] Elitas M, Demir B. Residual stress evaluation during RSW of DP600 sheet steel. Mater Test 2020;62:888–890. [CrossRef]

[5] Akulwar S, Akela A, Kumar DS, Ranjan M. Resistance spot welding behavior of automotive steels. Trans Indian Inst Metals 2021;74:601–609. [CrossRef]

[6] Rao SS, Arora KS, Sharma L, Chhibber R. Investigations on mechanical behaviour and failure mechanism of resistance spot-welded DP590 steel using artificial neural network. Trans Indian Inst Metals 2021;74:1419–1438. [CrossRef]
[7] Elitas M, Demir B. The effects of the welding parameters on tensile properties of RSW junctions of DP1000 sheet steel. Eng Technol Appl Sci Res 2018;8:3116–3120. [CrossRef]
[8] Hayat F, Demir B, Acarer M. Tensile shear stress and microstructure of low-carbon dual-phase Mn-Ni steels after spot resistance welding. Metal Sci Heat Treat 2007;49:484–489. [CrossRef]
[9] Baskoro AS, Muzakki H, Kiswanto G, Winarto W. Mechanical properties and microstructures on dissimilar metal joints of stainless steel 301 and aluminum alloy 1100 by micro-resistance spot welding. Trans Indian Inst Metals 2019;72:487–500. [CrossRef]
[10] Elitas M. Effects of welding parameters on tensile properties and failure modes of resistance spot welded DC01 steel. Proceed Inst Mech Eng Part E J Process Mech Eng 2023;37:1607–1616. [CrossRef]
[11] Shamsujjoha M, Enloe CM, Chuang AC, Coryell JJ, Ghassemi-Armaki H. Mechanisms of paint bake response in resistance spot-welded first and third generation AHSS. Materialia 2021;15:100975. [CrossRef]
[12] Onn IH, Ahmad N, Tamin MN. Fatigue characteristics of dual-phase steel sheets. JMech Sci Technol 2015;29:51–57. [CrossRef]
[13] Pal TK, Bhowmick K. Resistance spot welding characteristics and high cycle fatigue behavior of DP 780 steel sheet. J Mater Eng Perform 2012;21:280–285. [CrossRef]
[14] Oh G, Akiniwa Y. Bending fatigue behavior and microstructure in welded high-strength bolt structures. Proceed Inst Mech Eng C J Mech Eng Sci 2019;233:3557–3569. [CrossRef]
[15] Alzahougi A, Elitas M, Demir B. RSW Junctions of advanced automotive sheet steel by using different electrode pressures. Eng Technol Appl Sci Res 2018;8:3492–3495. [CrossRef]
[16] Khan MI, Kuntz ML, Biro E, Zhou Y. Microstructure and mechanical properties of resistance spot welded advanced high strength steels. Mater Trans 2008;49:1629–1637. [CrossRef]
[17] Ma C, Chen DL, Bhole SD, Boudreau G, Lee A, Biro E. Microstructure and fracture characteristics of spot-welded DP600 steel. Mater Sci Eng A 2008;485:334–346. [CrossRef]
[18] Pouranvari M, Marashi SPH. Critical review of automotive steels spot welding: process, structure and properties. Sci Technol Weld Join 2013;18:361–403. [CrossRef]
[19] Soomro IA, Pedapati SR, Awang M, Alam MA. Effects of double pulse welding on microstructure, texture, and fatigue behavior of DP590 steel resistance spot weld. Int J Adv Manuf Technol 2023;125:1271–1287. [CrossRef]
[20] Janardhan G, Dutta K, Mukhopadhyay G. Influence of work hardening on tensile and fatigue behavior of resistance spot-welded dual-phase steel. J Mater Eng Perform 2023;32:624–637. [CrossRef]
[21] Kishore K, Kumar P, Mukhopadhyay G. Microstructure, tensile and fatigue behaviour of resistance spot welded zinc coated dual phase and interstitial free steel. Metals Mater Int 2022;4:945–965. [CrossRef]
[22] Ghanbari HR, Shariati M, Sanati E, Nejad RM. Effects of spot welded parameters on fatigue behavior of ferrite-martensite dual-phase steel and hybrid joints. Eng Fail Anal 2022;134:106079. [CrossRef]]
[23] Xie L, Shi B, Xiao Z, Ren J, Li D. Fatigue characteristics of dp780 steel spot welding joints with different static fracture modes. Mater Trans 2021;62:191–197. [CrossRef]
[24] Ordoñez JH, Ambriz RR, García C, Plascencia G, Jaramillo D. Overloading effect on the fatigue strength in resistance spot welding joints of a DP980 steel. Int J Fatigue 2019;121:163–171. [CrossRef]
[25] Ordoñez Lara JH, Ambriz RR, García C, Plascencia G, Jaramillo D. Fatigue Life of Resistance Spot Welding on Dual-Phase Steels. In: Ambriz RR, Jaramillo D, Plascencia G, Nait Abdelaziz M, editors. Proceedings of the 17th International Conference on New Trends in Fatigue and Fracture, Cham: Springer International Publishing; 2018, p. 225–236. [CrossRef]
[26] Kumar KS, Ravikanth TN, Prashanth B, Sandeep CS. Experimental investigation on spot welding of mild, cold rolled steel and galvanised iron sheets. Int J Mech Eng Technol 2017;8:574–580.
[27] Babalık FC, Çavdar K. Machine Elements and Construction Examples. Bursa: DORA Publishing; 2013.
[28] Hambling SJ, Jones TB, Fourlaris G. Influence of steel strength and loading mode on fatigue properties of resistance spot welded H beam components. Mater Sci Technol 2004;20:1143–1150. [CrossRef]
[29] Bae DH, Sohn IS, Hong JK. Assessing the effects of residual stresses on the fatigue strength of spot welds. Weld J 2003;82:18–23.
[30] Rathbun RW, Matlock DK, Speer JG. Fatigue behavior of spot welded high-strength sheet steels. Weld J 2003;82:207–218.
[31] Hilditch TB, Speer J y, Matlock DK. Effect of susceptibility to interfacial fracture on fatigue properties of spot-welded high strength sheet steel. Mater Design 2007;28:2566–2576. [CrossRef]
[32] Long X, Khanna SK. Fatigue properties and failure characterization of spot welded high strength steel sheet. Int J Fatigue 2007;29:879–886. [CrossRef]

[33] Swellam MH, Aś GB, Lawrence FV. A fatigue design parameter for spot welds. Fatigue Fracture Eng Mater Struct 1994;17:1197–1204. [CrossRef]

[34] Long X, Khanna SK. Fatigue performance of spot welded and weld bonded advanced high strength steel sheets. Sci Technol Weld Join 2008;13:241–247. [CrossRef]

[35] Radaj D, Sonsino CM, Fricke W. Fatigue assessment of welded joints by local approaches. Cambridge: Woodhead Publishing; 2006. [CrossRef]

[36] Holovenko O, Ienco MG, Pastore E, Pinasco MR, Matteis P, Scavino G, et al. Microstructural and mechanical characterization of welded joints on innovative high-strength steels. La Metall Ital 2013;3:3–12.